JSR Publications

Available Online

J. Sci. Res. **18** (1), 11-28 (2026)

JOURNAL OF SCIENTIFIC RESEARCH

www.banglajol.info/index.php/JSR

Statistical Evaluation of a Heat Exchanger for Different Fluid Flow Parameters

B. Chowdhury[1*], S. K. Mohan[2], B. Saikia[1], P. P. Sahu[3]

[1]Department of Mechanical Engineering, Tezpur University, Tezpur 784028, India

[2]Monash Innovation Labs, Monash University, Melbourne, Australia

[3]Department of Electronics and Communication Engineering, Tezpur University, Tezpur -784028, India

Received 21 February 2025, accepted in final revised form 13 June 2025

Abstract

Heat exchangers are employed extensively in different industries such as ship building, chemical technology, power, food and beverage, and others. Maximum heat transfer in a heat exchanger is desired to achieve the highest possible efficiency and performance of the device. The heat transfer dynamics of a shell and tube heat exchanger with water as the heat transfer fluid are statistically examined in this study using the Full Factorial Design of Experiments approach. Input variables include the fluid flow parameters namely mass flow rates of the hot and cold water (50-250 L/h) as well as the temperature of the hot fluid entering (48.1-66 °C). The responses evaluated are the log mean temperature difference, heat transfer rate, effectiveness and overall heat transfer coefficient. The findings indicate that high flow rates and a high inlet temperature are the optimal input settings for maximum heat transfer. Low flow rates and high inlet temperature are the best settings for maximum effectiveness. The interactions between flow rates have a significant impact on the responses of heat transfer rate, overall heat transfer coefficient, and effectiveness. Effectiveness is also affected by the interaction of cold fluid's flow rate and its inlet temperature.

Keywords: Factor interactions; Log mean temperature difference; Effectiveness; Heat transfer; Statistical analysis; Design of experiments; Heat exchanger.

doi: https://dx.doi.org/10.3329/jsr.v18i1.79974 J. Sci. Res. **18** (1), 11-28 (2026)

1. Introduction

Heat exchanger devices are a common means of facilitating heat transfer from one fluid to another or recouping waste heat [1]. The analysis of the heat transfer performance of these devices is crucial for enhancing the process. Numerous methods are being applied for the analysis, considering a wide range of factors and parameters. The parameters considered are geometric, flow, and thermo-physical parameters that influence the heat transfer performance dynamics of a heat exchanger. Usually, the heat transfer dynamics of a heat

* *Corresponding author:* barnalidas@gmail.com

exchanger are explained using its log mean temperature difference (LMTD), effectiveness (Ɛ), heat transfer rate (Q) and overall heat transfer coefficient (U).

Experimental analysis of a heat transfer system is a basic method that involves investigating individual factors, leading to multiple experiments. Moreover, this approach is time-consuming and does not provide any scope to understand the interactions among the factors and their effects on the system's performance. These drawbacks of empirical analysis can be overcome by employing the statistical approach of full factorial design of experiments (DOE) [2]. The method uses a scientific approach to systematically plan experiments [3,4], examining a variety of input factors simultaneously and evaluating their impact on the desired outcome (response). Here mathematical models are developed and the effects of the individual factors and their interactions on the system's performance are identified which are otherwise missed in the one-factor-at-a-time (OFAT) experimental approach [5].

The analysis facilitates the optimization of the factors that influence the system's response [6]. In this work, full factorial DOE is employed to statistically investigate the impact of factors and their interactions on the heat transfer dynamics of a shell and tube heat exchanger, and formulate models for optimum heat transfer performance. The responses LMTD, Ɛ, Q and U are estimated by conducting designed experiments using the heat exchanger.

DOE applied to various heat exchanger problems for practical analysis and optimization in the current field of research supports to plan experiments and analyze the obtained results [5,7]. The growing advances of DOE enable the researchers to reduce the limitations of the traditional analysis methods, thus enhancing the quality of the analyses. The significance of design parameters of a heat exchanger is studied using the central composite DOE. Regression models are developed to comprehend the effect of process parameters on the responses. The inlet temperature of the hot fluid has a significant impact on heat transfer rate, whereas the mass flow rate of cold fluid affected effectiveness and pressure drop [8]. The Taguchi method of DOE is applied to study effect of design parameters in an overlapped helical baffled heat exchanger [9]; and effect of width and pitch of turbulators and Reynolds number (Re) of the flow on heat transfer performance of a turbulated heat exchanger [10]; Re, number of injectors and its design and arrangements that affect the heat transfer and pressure drop in a concentric heat exchanger [11]; in analyzing design and flow parameters namely Re, duct height and winglet length affecting the responses in a plate-fin heat exchanger [12]. A complete factorial experimental design approach is used to obtain the exergy efficiency of a double pipe heat exchanger with nanofluids and twisted tapes [13]; to observe interaction effects among the experimental parameters impacting heat transfer performance of a louvered fin compact heat exchanger [14]. With computational fluid dynamics, DOE is employed in a gas-solid fluidized bed heat exchanger to analyze and determine significant process parameters [15] impacting its heat transfer coefficient. The effectiveness and exit temperature of the cold fluid of a heat exchanger prototype are experimentally evaluated [16]; simulation programs are deployed to investigate the role of heat exchanger design on the efficiency of energy transfer and heat distribution for different

flow arrangements [17]. CFD and DOE are applied in the thermo-entropic analysis of a wavy twisted tri-lobed tube heat exchanger [18].

From the literature surveyed, it is observed that the studies mostly focus on the assembled type of heat exchangers with analysis mostly on design parameters. While a handful has been carried out on flow and thermal parameters that affect the heat transfer dynamics. Further, there has not been much emphasis on the statistical analysis of the most conventional type, 'the shell and tube heat exchanger.' The focus of the paper is therefore directed towards the statistical analysis of the process parameters (flow and thermal) of a shell and tube heat exchanger other than its design. The current research stresses on statistically evaluating the effect of input parameters, namely mass flow rates of hot and cold fluids and hot fluid temperature, on the heat transfer performance responses of a one-pass shell and tube heat exchanger. The important aspect of the study involves statistical analysis of the interactions among the input parameters and understanding their combined effect on the responses.

2. Methodology

This research work utilizes the Full Factorial Design of Experiments methodology because there are less than four process parameters with two levels for each parameter [6]. A full factorial experiment is a statistical experiment with two or more factors, each having discrete potential values or 'levels' [3]. The limitations of OFAT are overcome using the methodology. It allows for the analysis of the impact of each factor on the response variable, as well as the effects of interactions among factors on the response variable [6].

2.1. *Fixing the regression coefficients for input parameters*

The Full Factorial Design of Experiments is used to carry out the statistical evaluation of heat transfer responses of the heat exchanger. For a full factorial design of n factors, the response variable Z is represented by a linear regression polynomial [3] as in Eq. (1)

$$Z = d_0 + \sum_{i=1}^{n} d_i x_i + \sum_{i,j=1,j\neq i}^{n} d_{ij} x_i x_j + \sum_{i,j,k=1,k\neq j\neq i}^{n} d_{ijk} x_i x_j x_k \,, \quad (1)$$

where d_0, d_i, d_{ij} and d_{ijk} are regression coefficients and x_i, x_j, x_k are independent factors.

To investigate the heat transfer dynamics of the shell and tube heat exchanger and evaluate its performance, three input or process parameters, i.e., main factors, are considered. These input factors are the hot water flow rate (F_h), cold water flow rate (F_c), and the inlet temperature of the hot fluid (T_{h1}). Since the input parameters considered in this current work is less than four, so the Eq. (1) is rewritten as

$$Z = d_o + d_1 F_c + d_2 F_h + d_3 T_{h1} + d_{12} F_c F_h + d_{13} F_c T_{h1} + d_{23} F_h T_{h1} + d_{123} F_c F_h T_{h1}, \quad (2)$$

where F_c , F_h and T_{h1} represent the independent factors in Eq. (2). The multiple response variables considered in this research work are Z_1= LMTD, Z_2 = Ɛ, Z_3 = Q and Z_4= U.

2.2. *Developing the L_8 orthogonal experimental array*

To conduct the investigation using full factorial DOE, an L_8 orthogonal experimental array is developed for three factors A, B and C, respectively representing F_c , F_h and T_{h1}. Considering two levels for each factor, the full factorial DOE sample size is $2^3 = 8$, which results in eight designed experimental runs [4,19]. The design matrix for a 2^3 full factorial design that represents the L_8 orthogonal array for three input parameters is developed as shown in Table 1.

Table 1. Design matrix of 2^3 full factorial design.

	Factors							
		I	A	B	AB	C	AC	BC	ABC
Treatments	1	+	-	-	+	-	+	+	-
	a	+	+	-	-	-	-	+	+
	b	+	-	+	-	-	+	-	+
	ab	+	+	+	+	-	-	-	-
	c	+	-	-	+	+	-	-	+
	ac	+	+	-	-	+	+	-	-
	bc	+	-	+	-	+	-	+	-
	abc	+	+	+	+	+	+	+	+

Table 2. Factor levels.

Input variables	Low level	High level
F_c (L/h)	50	250
F_h (L/h)	50	250
T_{h1} (°C)	48.1	66

In Table 1, the signs '+' and '-' describe the upper and lower ranges for each independent variable. A, B and C are the main input factors while AB, AC, BC and ABC represent interactions among the input factors. The possible treatment combinations are 1, a, b, c, ab, ac, bc, abc [20]. The input factors F_c , F_h and T_{h1} influence the heat transfer output responses Z_1, Z_2, Z_3 and Z_4. Each factor has two levels, denoted by low and high range values. Table 2 provides the two levels of the input parameters. With the design matrix in Table 1 and factor levels in Table 2, the full factorial design matrix for the heat exchanger experiment is generated in the statistical solver MINITAB. The full factorial DOE is provided in Table 3. Experiments are performed for each of the eight designed experimental settings (Table 3) in the one-pass shell and tube heat exchanger (Fig. 1a). The responses LMTD, Ɛ, Q and U are obtained (Table 4) (Appendix A. Eq. A.1-A.14). There are no replications of the treatment combinations, so there is no replicated complete factorial design of experiment.

2.3. *Experiments*

The experimental set up of a shell and tube heat exchanger that has a tube fixed inside a high-speed steel (HSS) shell is illustrated in Fig. 1a. It has physical dimensions of shell

length (L) of 0.5 m, tube inner diameter (Di) of 0.013 m, and outer diameter (Do) of 0.016 m. The heat transfer process is accomplished by circulating hot fluid around a single-pass tube (Fig. 1b). The counter-flow heat exchanger circulates hot water inside an enclosed space called the shell, while cold water flows inside the single-pass tube spiralled around the shell's inner surface. The hot fluid in the shell warms the cold fluid in the tubes, while the cold liquid in the tube cools the warm fluid in the shell. The flow rates of both hot and cold water can be controlled by using valves. A magnetic drive pump fitted is used to circulate the hot water to the heat exchanger, and a digital temperature controller is used to control the water temperature. The temperatures of the fluids at various sensors are recorded after the flow reaches steady state.

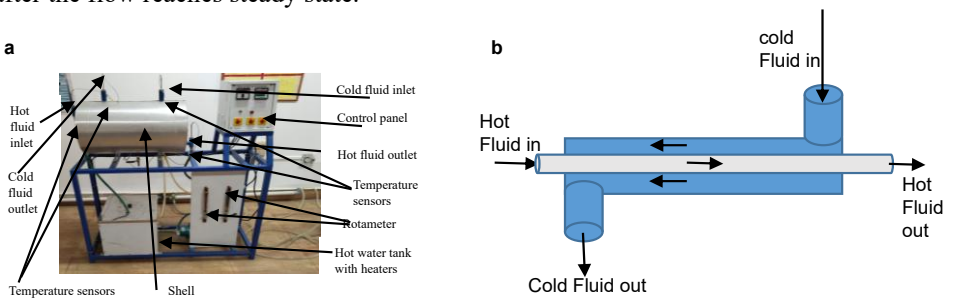

Fig. 1. (a) Experimental setup of the single pass shell and tube heat exchanger. (b) Schematic view of the heat exchanger.

Table 3. Full Factorial Design Matrix for the experiment.

Std order	Run Order	F_c (L/h)	F_h (L/h)	T_{h1} (°C)
1	8	50	50	48.1
2	4	250	50	48.1
3	2	50	250	48.1
4	5	250	250	48.1
5	7	50	50	66.0
6	3	250	50	66.0
7	6	50	250	66.0
8	1	250	250	66.0

Table 4. Heat transfer responses of full factorial DOE.

Std order	Run order	LMTD (°C)	Ɛ	Q (W)	U (W/m^2 K)
1	8	11.94	0.71	616.84	2055.54
2	4	11.91	0.73	782.25	2612.44
3	2	15.65	0.38	1730.08	1730.08
4	5	15.81	0.38	2205.24	5549.17
5	7	20.61	0.70	1526.30	2946.61
6	3	19.91	0.75	1553.91	3105.38
7	6	25.31	0.56	2341.89	3681.58
8	1	27.74	0.37	4294.25	6159.44

2.4. *Model Formulation*

The heat transfer performances (Table 4) are statistically evaluated to estimate the effects of factors and their interactions on the responses (Appendix A. Tables A.1-A.4). The coefficients for each response are shown in Table 5. The mathematical modelling of the responses LMTD, Ɛ, Q and U obtained using the regression coefficients (Table 5) are represented by equations Eqs. (3) to (6) respectively.

Table 5. Regression coefficients.

Factors (corresponding coefficients)	Coefficients for			
	LMTD	ε	Q	U
Constant (d_0)	18.61	0.57	1881.30	3480.00
F_c (d_1)	0.23	-0.01	327.60	876.60
F_h (d_2)	2.52	-0.15	761.50	800.00
T_{h1}(d_3)	4.78	0.02	547.70	493.20
F_c*F_h (d_{12})	0.42	-0.03	279.30	697.70
F_c*T_{h1} (d_{13})	0.20	-0.02	167.40	-217.40
F_h*T_{h1} (d_{23})	0.62	0.02	127.50	147.20
F_c*F_h*T_{h1} (d_{123})	0.37	-0.03	201.90	-117.90

Table 6. p-values of significant factors.

Significant factors	p-values of			
	LMTD	ε	Q	U
Constant	0.00	0.00	0.00	0.00
F_c	0.51	0.58	0.15	0.01
F_h	0.01	0.01	0.02	0.02
T_{h1}	0.00	0.41	0.05	0.06
F_c*F_h	0.30	0.27	0.20	0.03
F_c*T_{h1}	-	-	-	-
F_h*T_{h1}	0.17	-	-	-

$$\text{LMTD} = 18.61 + 0.23F_c + 2.52F_h + 4.78T_{h1} + 0.42\,F_cF_h + 0.20F_cT_{h1} + 0.62F_hT_{h1} + 0.37F_cF_h\,T_{h1} \quad (3)$$

$$\text{Ɛ} = 0.57 - 0.01F_c - 0.15F_h + 0.02T_{h1} - 0.03F_cF_h - 0.02F_cT_{h1} + 0.02F_hT_{h1} - 0.03F_cF_hT_{h1} \quad (4)$$

$$\text{Q} = 1881.30 + 327.60F_c + 761.50F_h + 547.70T_{h1} + 279.30F_cF_h + 167.40F_cT_{h1} + 127.50F_hT_{h1} + 201.90F_cF_hT_{h1} \quad (5)$$

$$\text{U} = 3480.00 + 876.60F_c + 800\,F_h + 493.20T_{h1} + 697.70F_cF_h - 217.40F_cT_{h1} + 147.20F_hT_{h1} - 117.90F_cF_hT_{h1} \quad (6)$$

Equations Eqs. (3) to (6) show the values of model coefficients. But for estimating the significant effect of factors on responses, 'analysis of variance' (ANOVA) is conducted at a 5 % level of significance. Before ANOVA, the sparsity of effects principle [3,5,14] is applied, and higher order 3-way interactions dropped from the models as these have negligible significance on heat transfer performance. The subsequent higher degree terms are also removed from the analysis one at a time. Table 6 displays the significant parameters and p-values (P) of the corresponding effects for each response. The final P of interaction effects with negligible significance on the responses is excluded.

3. Results and Discussion

3.1. *Determining significant factors*

The significant factors of heat transfer performance are obtained from the analysis of variance of the factors' effects (Appendix A. Tables A.5-A.8). The hypothesis for the analysis is established as follows:

H_0: Factor Effect is insignificant (P>0.05)

H_1: Factor Effect is significant.

3.1.1. *Analysis of LMTD*

The ANOVA of LMTD (Appendix A. Table A.5) shows that F_h and T_{h1} have a significant effect with P < 0.05 (Table 6). The model includes interaction terms $F_c * F_h$ and $F_h * T_{h1}$, although the P > 0.05. These interaction terms influence the response in comparison to the removed higher order interaction terms due to the presence of F_h and T_{h1}. Furthermore, keeping the interaction terms help improve the model by increasing the value of adjusted-R^2 (Table 8). F_c has a P> 0.05 (Table 6) but is considered in the final model of LMTD due to its theoretical and practical importance.

The normal probability plot for LMTD (Fig. 2a) obtained from ANOVA also indicates that F_h and T_{h1} are crucial factors that have a positive impact on the response. The Pareto Chart (Fig. 2b) identifies F_h and T_{h1} as strongly influencing the response and T_{h1} is the most effective. The main effects plot (Fig. 2c) reveals an increase in LMTD with both F_h and T_{h1}, while the increase in F_c has minimal significance. The interaction effects plot of LMTD (Fig. 2d) illustrates the negligible significance of interactions on LMTD. It is also apparent from the ANOVA that the interactions are not statistically significant. Fig. 2d provides the evidence of this fact as in the plots the lines are almost parallel to each other and have the same slope.

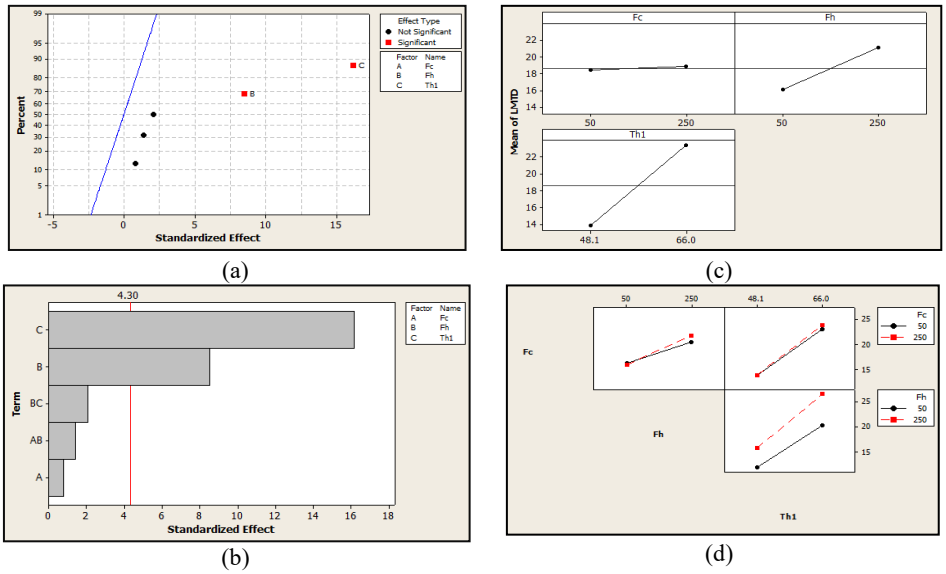

Fig. 2. Analysis of LMTD. (a) Normal probability plot of the effects. (b) Pareto chart of the effects. (c) Main effects plot. (d) Interaction effects plot.

3.1.2. *Analysis of* Ɛ

The significant parameter in ANOVA of Ɛ (Appendix A. Table A.6) is F_h, which has a P of 0.01 (Table 6). The other individual terms F_c and T_{h1} are included in the model due to their theoretical importance, regardless of having a P>0.05 (Table 6). The interaction term F_c* F_h is retained in the model because removing it decreases the adjusted-R^2 value from 84.74 % to 81.72 %. The model provides a fair amount of R^2 and adjusted-R^2 (Table 8).

The normal probability plot for Ɛ (Fig. 3a) indicates that F_h is the most significant factor and has a negative effect on the response. F_h is identified as the most significant parameter by the Pareto analysis (Fig. 3b). The main effects plot (Fig. 3c) describes the decrease of Ɛ with the increase in F_h, whereas the influence of F_c and T_{h1} on Ɛ is relatively less substantial. The interaction plot (Fig. 3d) reveals that the significant interactions are F_c * F_h and F_c * T_{h1}. There is no significant effect for the interaction term F_h* T_{h1}, so it was dropped from the modified regression model.

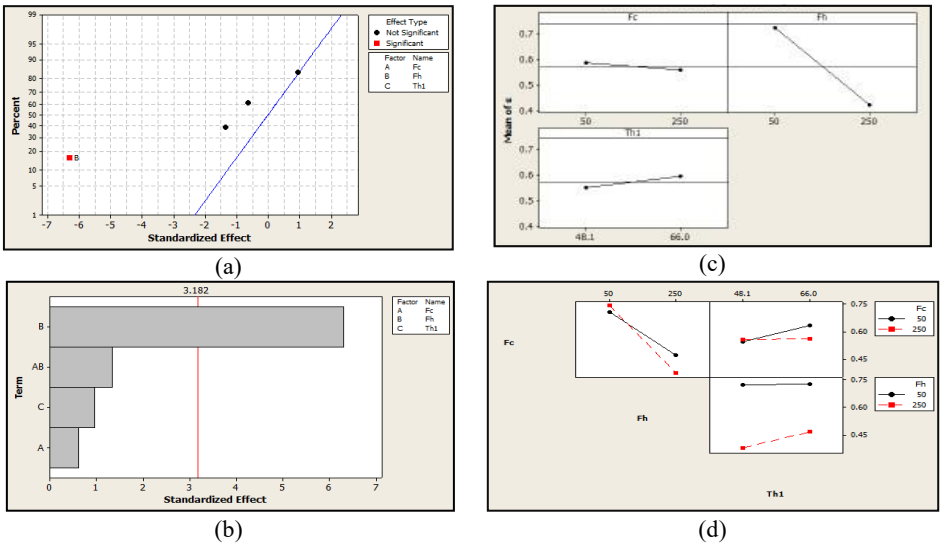

Fig. 3. Analysis of Ɛ. (a)Normal probability plot of the effects. (b) Pareto chart of the effects. (c) Main effects plot. (d) Interaction effects plot.

3.1.3. *Analysis of* Q

The most important parameter obtained in the variance analysis of Q (Appendix A. Table A.7) is F_h due to a P of 0.02 (Table 6). The subsequent significant parameter is T_{h1}, which has a P of 0.05. F_c is not statistically significant but is retained in the model due to its practical importance. The interaction term F_c* F_h is also included as its removal reduces the adjusted-R^2 from 82.75 % to 75.19 %. The final regression model thus improves the value of adjusted-R^2 (Table 8).

Further graphical analysis was carried out using a normal probability plot to analyze the effects of the factors. Fig. 4a reveals F_h and T_{h1} as the significant factors influencing Q, and their effect on the output is positive. The Pareto chart (Fig. 4b) also identifies that F_h and T_{h1} are relevant to the system. The main effects plot (Fig. 4c) reveals a significant increase in Q along with the increase in both F_h and T_{h1}, while the increase in F_c is not as significant. The interaction plot (Fig. 4d) shows F_c * F_h as the significant interaction compared to the other two-way interactions.

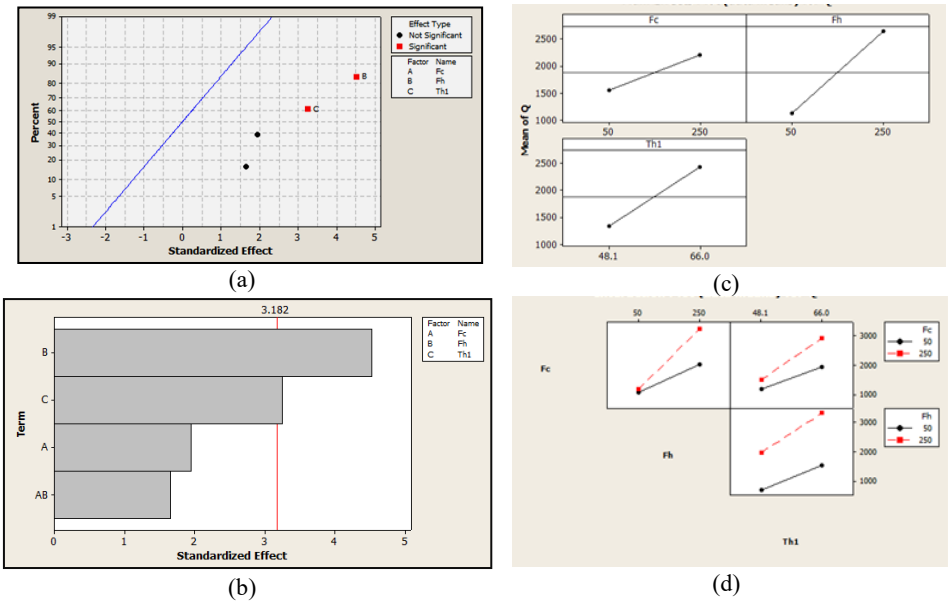

Fig. 4. Analysis of Q. (a) Normal probability plot of the effects. (b) Pareto chart of the effects. (c) Main effects plot. (d) Interaction effects plot.

3.1.4. *Analysis of U*

The analysis of U (Appendix A. Table A.8) shows that the most significant parameter is F_c with a P value of 0.01 (Table 6). The succeeding relevant parameter is F_h with a P of 0.02, followed by F_c * F_h (P is 0.03) (Table 6). The T_{h1} is included in the final model because its removal drastically reduces the adjusted R^2 value from 91.30 % to 74.31 %. The model thus provides a satisfactory result of R^2 = 96.27 % and adjusted-R^2 = 91.30 %, with the regression line representing almost all of the data (Table 8).

The normal probability plot U in Fig. 5a demonstrates that F_c , F_h and the interaction term F_c * F_h are significant factors influencing the response. They have a positive impact on the output. The Pareto chart in Fig. 5b also shows that F_c , F_h and F_c * F_h are the crucial terms. The main effects plot of U (Fig. 5c) shows that U increases significantly with an increase in both F_c and F_h, while the rise of T_{h1} is the least significant. The interaction

effects plot in Fig. 5d reveals that the interaction F_c * F_h is significant compared to the terms F_c * T_{h1} and F_h* T_{h1}.

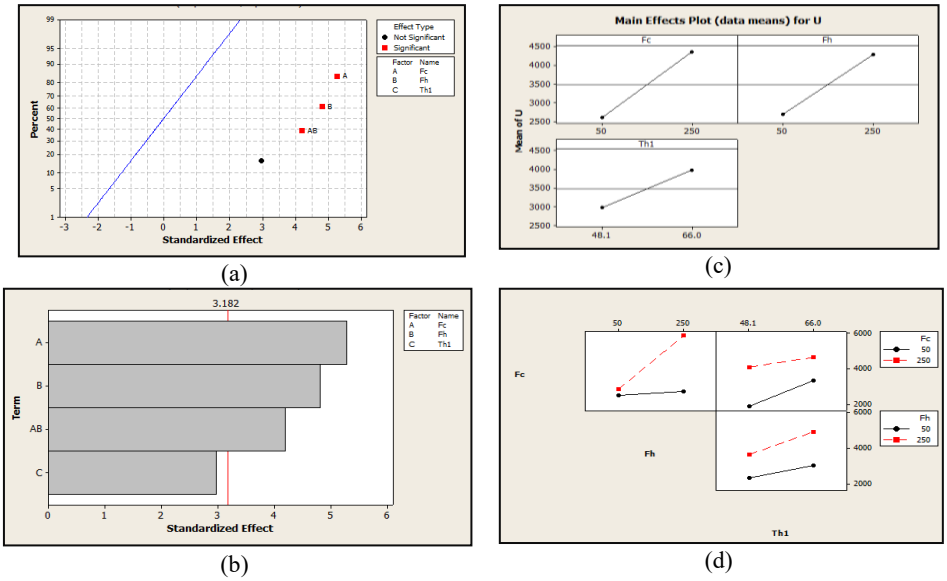

Fig. 5. Analysis of U. (a)Normal probability plot of the effects. (b) Pareto chart of the effects. (c) Main effects plot. (d) Interaction effects plot.

3.2. *Final regression models and residual analysis*

The final mathematical models of the responses LMTD, Ɛ, Q and U are formulated [Eq. (7) - (10)] with significant factors and respective regression coefficients (Table 5).

$$\text{LMTD} = 18.61 + 0.23F_c + 2.52\ F_h + 4.78\ T_{h1} + 0.42\ F_cF_h + 0.62\ F_hT_{h1}, \quad (7)$$

$$\text{Ɛ} = 0.57 - 0.01F_c - 0.15\ F_h + 0.02\ T_{h1} - 0.03\ F_cF_h\ , \quad (8)$$

$$\text{Q} = 1881.30 + 327.60\ F_c + 761.50\ F_h + 547.70\ T_{h1} + 279.30\ F_cF_h\ , \quad (9)$$

$$\text{U} = 3480.00 + 876.60\ F_c + 800\ F_h + 493.20\ T_{h1} + 697.70\ F_cF_h\ , \quad (10)$$

Using the regression models [Eqs. (7)-(10)], the predicted responses are calculated (Table 7). The R^2 and adjusted-R^2 obtained due to regression of the responses (Table 8), signify good fit of the experimental data with the statistically developed regression models [21]. The R^2 for the responses explain the precision of the linear models [Eqs. (3)-(6)]. However, as the sensitivity of R^2 increases with increase in number of independent terms and from ANOVA as the insignificant model input factors are dropped, adjusted-R^2 value validates the model adequacy. This corrected R^2 value, which is slightly less than R^2, represents the exact number of significant input parameters in the models [22]. For a model to indicate good fit, the value of R^2 and adjusted-R^2 should be more than 80 % [23-25]. Consequently, in the present investigation, the values of adjusted-R^2 for the multiple

responses were above 80 % (Table 8), indicating adequate fit of the behavior of the responses with the statistical models.

Table 7. Observed and predicted values of the multiple responses.

Full Factorial Design of experiments					Responses of Full Factorial DOE							
					Observed				Predicted			
SN	Run Order	F_c (L/h)	F_h (L/h)	T_{h1} (°C)	LMTD (°C)	Ɛ	Q (W)	U W/m^{2}K)	LMTD (°C)	Ɛ	Q (W)	U (W/m^{2}K)
1	8	50	50	48.10	11.94	0.71	616.84	2055.54	14.37	0.48	523.79	2007.90
2	4	250	50	48.10	11.91	0.73	782.25	2612.44	14.01	0.51	620.39	2365.70
3	2	50	250	48.10	15.65	0.38	1730.08	1730.08	17.35	0.24	1488.19	2212.50
4	5	250	250	48.10	15.81	0.38	2205.24	5549.17	18.64	0.15	2701.99	5361.10
5	7	50	50	66.00	20.61	0.70	1526.3	2946.61	18.18	0.93	1619.21	2994.30
6	3	250	50	66.00	19.91	0.75	1553.91	3105.38	17.81	0.97	1715.81	3352.10
7	6	50	250	66.00	25.31	0.56	2341.89	3681.58	23.61	0.70	2583.61	3198.90
8	1	250	250	66.00	27.74	0.37	4294.25	6159.44	24.91	0.60	3797.41	6347.50

Table 8. R^2 and adjusted-R^2 values for model validation.

Responses	R^2 (%)	Adjusted-R^2 (%)
LMTD	99.42	97.96
Ɛ	93.46	84.74
Q	95.04	82.66
U	96.27	91.30

3.2.1. *Residual analysis*

The normal probability plot of residuals of LMTD, Ɛ, Q and U (Appendix A. Fig. A.1 (a-d)), respectively reveal that the errors are almost normally distributed in the experiment. The scatter plots of the responses (Appendix A. Fig. A.2 (a-d)) do not show any specific pattern that indicates constant variance of the residuals. The errors between the predicted and experimental heat transfer performance outputs are independent and follow a normal distribution. Based on the residual analysis, it can be concluded that the optimized models fit the observed data of heat transfer responses sufficiently at a 5 % level of significance.

3.3. *Optimized factors*

Table 9 shows the optimized input factors A, B, C set at high level for the heat transfer responses LMTD, Q and U. Whereas Table 10 shows the optimized factors for Ɛ, indicating optimum values of factors A and B at lower rates and factor C at higher value. It has been observed that the dynamics of LMTD, Q and U increase with an increase in F_c, F_h and T_{h1}. Hence, the heat exchanger should be operated at higher level of the input parameters, i.e., fluid flow rates at 250 L/h with T_{h1} at 66 °C to maximize the outputs LMTD, Q and U. The effect of Ɛ decreases with an increase in F_c and F_h , and it increases with an increase in T_{h1}. To optimize Ɛ, the heat exchanger should operate at the lower flow rates, which is 50 L/h, with T_{h1} at 66 °C.

Table 9. Optimized input parameters fo LMTD, Q and U.

Factors	Process parameter	Optimum setting	Optimized values
Factor A	F_c	High	250 L/h
Factor B	F_h	High	250 L/h
Factor C	T_{h1}	High	66 °C

Table 10. Optimized input parameters with Ɛ as the response.

Factors	Process parameter	Optimum setting	Optimized values
Factor A	F_c	Low	50 L/h
Factor B	F_h	Low	50 L/h
Factor C	T_{h1}	High	66 °C

By using the full factorial DOE optimization technique, process parameters optimized from the L_8 orthogonal array assessment are used to achieve the most favorable heat transfer responses (Appendix A. Table A.9).

4. Conclusion

This work statistically analyses the heat transfer performance dynamics of a single pass shell and tube heat exchanger based on the complete factorial DOE approach.
The effects of hot and cold fluids' flow rates and inlet temperature of the hot fluid on LMTD, U, Q and Ɛ are statistically observed. The impacts of factor interactions on the output responses are also analyzed. The significance of the parameters is quantified in terms of p-values obtained from ANOVA. The graphical analysis of normal probability and Pareto is performed to qualitatively illustrate the parameters' significance. The process parameters F_h and T_{h1} have a higher impact on LMTD and Q, whereas F_c and F_h are the vital parameters that influence U, and F_h is the most dominant factor in the optimization of Ɛ. The interaction $F_c * F_h$ significantly impacts Q, U and Ɛ. The effect of the interaction $F_c * T_{h1}$ is noticeable on the response Ɛ. However, the interaction terms have negligible significance on LMTD.
In case of LMTD, Q and U, the fluid flow rates are optimized at 250 L/h, with T_{h1} at 66 °C. Whereas for Ɛ, the optimized values of fluid flow rates are 50 L/h each with T_{h1} at the same value. The statistically developed predictor models with full factorial DOE at 5% level of significance resulted in maximization of LMTD at 24.91°C, Q at 3797.41 W and U at 6347.50 W/m^2 K, and optimization of Ɛ at 0.93 achieved at the optimized values of the input variables. The model validation with adjusted-R^2 was found to be greater than 80% indicating close proximity of the observed with the predicted responses. Residual analysis of the error between the predicted and observed responses reveals that the errors follow a normal distribution and are independent, signifying adequate fit of the models with the experimental data.

Appendix A.

The detailed analysis of full factorial DOE is presented in the Appendix. The equations pertaining to various calculations related to the heat transfer responses are provided. The preliminary estimation of effects and coefficients of the input parameters with various analyses leading to final estimation, which are part of the ANOVA, are documented here. Various graphical analysis associated with model validation are also covered. The supplementary also provides the optimized responses obtained from the predicted models. All the analysis involved in the work is carried out in the MINITAB.

A.1. Governing equations

Various governing equations are used in the calculation of the heat transfer performance responses of the shell and tube heat exchanger. The LMTD for counter flow arrangement of the heat exchanger is calculated using (A.1)

$$\text{LMTD} = \frac{\Delta T_1 - \Delta T_2}{\left(ln\frac{\Delta T_1}{\Delta T_2}\right)} \quad \text{(A.1)},$$

where, $\Delta T_1 = T_{h,1} - T_{c,2}$ and $\Delta T_2 = T_{h,2} - T_{c,1}$,
and $T_{h,1}$= inlet temperature of hot fluid, $T_{h,2}$= outlet temperature of hot fluid, $T_{c,1}$ = inlet temperature of cold fluid, $T_{c,2}$= outlet temperature of cold fluid.
The mass flow rate of hot water (m_h) is calculated using (A.2)

$$m_h = \frac{F_h \text{ X } \rho_h}{3600 \text{ X } 1000} \quad \text{(A.2)}$$

The mass flow rate of cold water (m_c) is calculated using (A.3)

$$m_c = \frac{F_c \text{ X } \rho_c}{3600 \text{ X } 1000} \quad \text{(A.3)}$$

where, F_h and F_c are the flow rates in L/h of hot and cold water, respectively. ρ_h is the density of hot water at T_h and T_h is given by (A.4)

$$T_h = \frac{T_{h,1} + T_{h,2}}{2} \quad \text{(A.4)}$$

ρ_c is the density of cold water at T_c and T_c is given by (A.5)

$$T_c = \frac{T_{c,1} + T_{c,2}}{2} \quad \text{(A.5)}$$

The heat transfer rate from the cold fluid is calculated using (A.6)

$$Q_c = m_c C_{pc}(T_{c,2} - T_{c,1}) \quad \text{(A.6)},$$

where, C_{pc} is the specific heat capacity of cold fluid.
The heat transfer rate from the hot fluid is calculated using (A.7)

$$Q_h = m_h C_{ph}(T_{h,1} - T_{h,2}) \quad \text{(A.7)},$$

where, C_{ph} is the specific heat capacity of hot fluid.
In ideal cases, the heat transfer rates Q_c and Q_h are equal, whereas in non-ideal cases, the average of Q_c and Q_h is calculated to determine the overall heat transfer rate. Thus, the overall heat transfer rate Q is obtained using (A.8),

$$Q = \frac{Q_h + Q_c}{2} \quad \text{(A.8)}$$

Again, Q expressed in terms of LMTD using (A.9),

$$Q = UA(\Delta T_m) \quad \text{(A.9)},$$

where *(ΔTm)* is the LMTD determined using (A.1), A is the area of the heat exchanger and

is calculated as $A = \pi D_o L$. Thus, the overall heat transfer coefficient can be determined using (A.10)

$$U = \frac{Q}{A\Delta T_m} \tag{A.10}$$

The ε of the heat exchanger is defined as,

$$\varepsilon = \frac{\text{actual heat transfer rate}}{\text{Maximum possible heat transfer rate}} \tag{A.11}$$

Mathematically, $\varepsilon = \frac{Q}{Q_{max}}$ (A.12)

Determining Q using (A.9) and Q_{max} by (A.13), ε is calculated using (A.14)

$$Q_{max} = C_{min}(T_{h,1} - T_{c,1}) \tag{A.13}$$

Therefore, ε is calculated as

$$\varepsilon = \frac{C_{ph}(T_{h,1}-T_{h,2})}{C_{min}(T_{h,1}-T_{c,1})} = \frac{C_{pc}(T_{c,2}-T_{c,1})}{C_{min}(T_{h,1}-T_{c,1})} \tag{A.14}$$

A.2. Supplementary tables

The ground work of ANOVA that estimated the effects of all the independent variables and their corresponding coefficients are represented in Tables A.1-A.4. Since there is no p-value provided in the estimated values in this preliminary investigation, the significant effects of the factors are not known. Sparsity of effects principle [3,5,14] is applied and three-way interaction terms are dropped from the models. Variance analyses at 5% level of significance for the remaining independent factors are carried out and regression models are developed. Tables A.5-A.8 show the estimated effects of the input variables with their corresponding coefficients and p-values.

Table A.1. Factorial Fit: LMTD Vs Input Parameters: Effects and Coefficients.

Term	Effect	Coefficient
Constant		18.61
F_c	0.46	0.23
F_h	5.03	2.52
T_{h1}	9.56	4.78
$F_c * F_h$	0.83	0.42
$F_c * T_{h1}$	0.40	0.20
$F_h * T_{h1}$	1.23	0.62
$F_c * F_h * T_{h1}$	0.74	0.37

Table A.2. Factorial Fit: ε Vs Input Parameters: Effects and Coefficients

Term	Effect	Coefficient
Constant		0.57
F_c	-0.03	-0.02
F_h	-0.30	-0.15
T_{h1}	0.05	0.02
$F_c * F_h$	-0.06	-0.03
$F_c * T_{h1}$	-0.04	-0.02
$F_h * T_{h1}$	0.04	0.02
$F_c * F_h * T_{h1}$	-0.06	-0.03

Table A.3: Factorial Fit: Q Vs Input Parameters: Effects and Coefficients

Term	Effect	Coefficient
Constant		1881.30
F_c	655.10	327.60
F_h	1523.00	761.50
T_{h1}	1095.50	547.70
$F_c * F_h$	558.60	279.30
$F_c * T_{h1}$	334.80	167.40
$F_h * T_{h1}$	254.90	127.50
$F_c * F_h * T_{h1}$	403.80	201.90

Table A.4: Factorial Fit: U Vs Input Parameters: Effects and Coefficients

Term	Effect	Coefficient
Constant		3480.00
F_c	1753.20	876.60
F_h	1600.10	800.00
T_{h1}	986.40	493.20
$F_c * F_h$	1395.30	697.70
$F_c * T_{h1}$	-434.80	217.40
$F_h * T_{h1}$	294.40	147.20
$F_c * F_h * T_{h1}$	-235.80	-117.90

Table A.5: ANOVA for LMTD (final model)

Term	Effect	Coefficient	SE	T	P
Constant		18.61	0.30	62.98	0.00
F_c	0.46	0.23	0.30	0.79	0.51
F_h	5.03	2.52	0.30	8.52	0.01
T_{h1}	9.56	4.78	0.30	16.18	0.00
$F_c * F_h$	0.83	0.42	0.30	1.40	0.30
$F_h * T_{h1}$	1.23	0.62	0.30	2.08	0.17
S = 0.84	R^2 = 99.42%		R^2 (adj) = 97.96%		

Table A.6: ANOVA for ε (final model)

Term	Effect	Coefficient	SE	T	P
Constant		0.57	0.30	24.02	0.00
F_c	-0.03	-0.02	0.20	-0.62	0.60
F_h	-0.30	-0.15	0.20	-6.31	0.01
T_{h1}	0.05	0.02	0.20	0.96	0.41
$F_c * F_h$	-0.07	-0.03	0.20	-1.34	0.27
S = 0.07	R^2 = 93.46%		R^2 (adj) = 84.74%		

Table A.7: ANOVA for Q (final model)

Term	Effect	Coeff	SE	T	P
Constant		1881.30	168.40	11.17	0.00
F_c	655.10	327.60	168.40	1.95	0.15
F_h	1523.00	761.50	168.40	4.52	0.02
T_{h1}	1095.50	547.70	168.40	3.25	0.05
$F_c * F_h$	558.60	279.30	168.40	1.66	0.20
S= 477.50	R^2 = 95.04%		R^2 (adj) = 82.66%		

Table A.8: ANOVA for U (final model)

Term	Effect	Coeff	SE	T	P
Constant		3480.00	166.20	20.94	0.00
F_c	1753.20	876.60	166.20	5.27	0.01
F_h	1600.10	800.00	166.20	4.81	0.02
T_{h1}	986.40	493.20	166.20	2.97	0.06
$F_c * F_h$	1395.30	697.70	166.20	4.20	0.03
S = 470.02	R^2 = 96.27%		R^2 (adj) = 91.30%		

A.3. Supplementary figures

The regression models Eqs. (7) to (10) obtained are validated by residual analysis. Figs. A.1 (a-d) and A.2 (a-d) illustrate the normal probability and scatter plots of errors associated with the predicted response parameters.

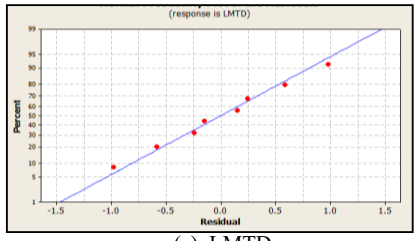

(a) LMTD

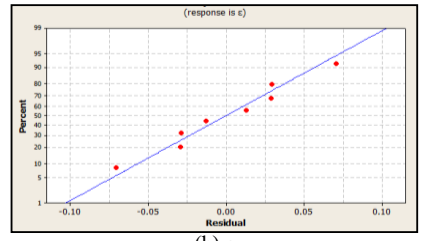

(b) ε

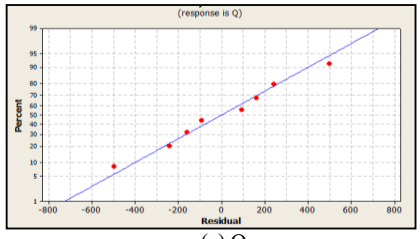

(c) Q

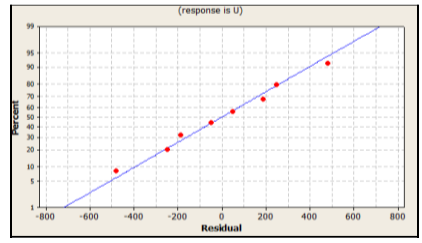

(d) U

Fig.A.1 (a-d). Normal probability plots of residuals

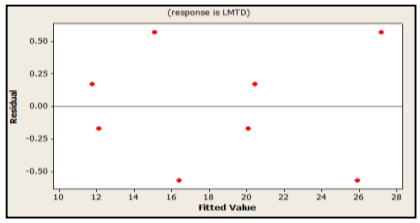

(a) LMTD

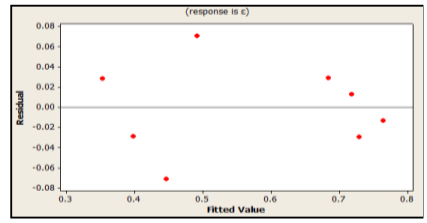

(b) ε

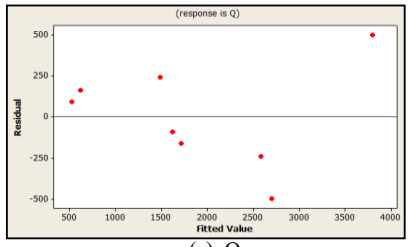

(c) Q

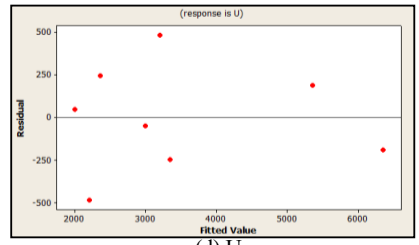

(d) U

Fig.A.2 (a-d). Scatter plots of error variances

A.4. Calculation of optimal heat transfer responses

Using the optimized values of the independent variables (from Tables 9 and 10), the optimal heat transfer responses namely LMTD, ε, Q and U are obtained (shown in Table A.9).

Table A.9: Optimal responses of the predictors

Optimal Responses			
LMTD (°C)	Q (W)	U ($W/m^2 K$)	E
24.91	3797.41	6347.5	0.93

References

1. J. H. Lienhard IV and J. H. Lienhard V, A Heat Transfer Textbook, 5th Edition (Phlogiston Press, Cambridge, UK, 2019).
2. R. Mee, A comprehensive Guide to Factorial Two-level Experimentation (Springer Science & Business Media, 2009). https://doi.org/10.1007/b105081
3. D. C. Montgomery, Design and analysis of Experiments, 8th Edition (John Wiley & Sons, 2017).
4. B. Chowdhury and S. K. Deb, Optimizing Thermoforming of Refrigerator Liners to Reduce Liner Rejection Rate - A Case Study Using Fractional Factorial Design of Experiments, in Advances in Mechanical Engineering, Lecture Notes in Mechanical Engineering, ed. G. Manik et al. (Springer, Singapore, 2021) pp. 225-238. https://doi.org/10.1007/978-981-16-0942-8_21
5. H. Toutenburg, S. Shalabh, and H. Shalabh, Statistical Analysis of 2^3 DOE, in Statistical Analysis of Designed Experiments, 3rd Edition (Springer-Verlag, New York, 2009) pp. 209-304. https://doi.org/10.1007/978-1-4419-1148-3
6. J. Antony, Design of experiments for engineers and scientists, 2nd Edition (Elsevier, 2014).
7. C. Ezgi, Basic Design Methods of Heat Exchanger. Heat Exchangers- Design, Experiment and Simulation, 9 (Intechopen, London, UK, 2017). https://doi.org/10.5772/67888
8. S. Balamurugan and D. Samsoloman, J. Heat Mass Trans. Res. **1**, 59 (2014).
9. T. Du, W. Du, K. Che and L. Cheng, Appl. Thermal Eng. **85**, 334 (2015). https://doi.org/10.1016/j.applthermaleng.2015.02.058
10. N. Celik, G. Pusat, and E. Turgut, Int. J. Thermal Sci. **124**, 85 (2018). https://doi.org/10.1016/j.ijthermalsci.2017.10.007
11. E. Turgut, G. Çakmak, and C. Yıldız, Energy Conv. Manag. **53**, 268 (2012). https://doi.org/10.1016/j.enconman.2011.09.011
12. I. Kotcioglu, A. Cansiz, and M. Khalaji, Appl. Thermal Eng. **50**, 604 (2013). https://doi.org/10.1016/j.applthermaleng.2012.05.036
13. H. Maddah, R. Aghayari, M. Mirzaee, M. Ahmadi, M. Sadeghzadeh, and A. Chamkha, Int. Commun. Heat Mass Transf. **97**, 92 (2018). https://doi.org/10.1016/j.icheatmasstransfer.2018.07.002
14. B. Ameel, J. Degroote, H. Huisseune, J. Vierendeels, and M. De Paepe, Int. J. Heat Mass Transf. **77**, 247 (2014). https://doi.org/10.1016/j.ijheatmasstransfer.2014.04.073
15. P.C. Bisognin, J. Bastos, H. Meier, N. Padoin, and C. Soares, Chem. Eng. Processing-Process Intensif. **147**, ID 107693 (2020). https://doi.org/10.1016/j.cep.2019.107693
16. C. Ramírez-Dolores, J. Andaverde, L. Ordoñez-Castillo, and J. Wong-Loya, Model. Exp. Des. **7**, 4117 (2024). https://doi.org/10.1007/s41939-024-00460-0
17. S. S. Alrwashdeh, H. Ammari, M. A. Madanat, and A.M. Al-Falahat, Emerging Sci. J. **6**, 128 (2022). https://doi.org/10.28991/ESJ-2022-06-01-010
18. S. Hadibafekr, I. Mirzaee, M. Khalilian, and H. Shirvani, Int. J. Therm. Sci. **184**, ID 107921 (2023). https://doi.org/10.1016/j.ijthermalsci.2022.107921
19. A. Jankovic, G. Chaudhary, and F. Goia, Energy Buildg. **250**, ID 111298 (2021). https://doi.org/10.1016/j.enbuild.2021.111298
20. G. W. Oehlert, A First Course in Design and Analysis of Experiments (Macmillan Learning, 2010).

21. B. R. Kumar, S. Saravanan, D. Rana, and A. Nagendran, Energy Convers. Manag. **123**, 470 (2016). https://doi.org/10.1016/j.enconman.2016.06.064
22. A. Glyk, D. Solle, T. Scheper, and S. Beutel, Chemom. Intell. Lab. Syst. **149**, 12 (2015). https://doi.org/10.1016/j.chemolab.2015.09.014
23. C. Buratti, M. Barbanera, E. Lascaro, and F. Cotana, Waste Manag. **73**, 523 (2018). https://doi.org/10.1016/j.wasman.2017.04.012
24. S. Bajar, A. Singh, C.P. Kaushik, and A. Kaushik, Waste Manag. **53**, 136 (2016). https://doi.org/10.1016/j.wasman.2015.09.023
25. H. Lou, W. Li, C. Li, and X. Wang, J. Appl. Polym. Sci. **130**, 1383 (2013). https://doi.org/10.1002/app.39317